Heliyon 9 (2023) e21169

Contents lists available at ScienceDirect

Heliyon

journal homepage: www.cell.com/heliyon

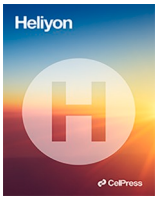

Chitosan-Based metal-organic framework for Stabilization of β-glucosidase: Reusability and storage stability☆

Mustafa Zeyadi [a], Yaaser Q. Almulaiky [b,c,*]

[a] Department of Biochemistry, Faculty of Science, King Abdulaziz University, Jeddah, P. O. Box 80200, Jeddah, 21589, Saudi Arabia
[b] Department of Chemistry, College of Science and Arts at Khulis, University of Jeddah, Jeddah 21921, Saudi Arabia
[c] Chemistry Department, Faculty of Applied Science, Taiz University, Taiz, Yemen

ARTICLE INFO

Keywords:
β-glucosidase
Immobilization
Metal-organic frameworks
Stability
Reusability

ABSTRACT

Enzyme immobilization is a powerful tool for protecting enzymes from harsh reaction conditions and improving enzyme activity, stability, and reusability. In this study, metal organic frameworks (MIL-Fe composites) were synthesized via solvothermal reactions and then modified with chitosan (CS). β-Glucosidase was immobilized on the chitosan-metal organic framework (CS-MIL-Fe), and the resulting composites were characterized with various analytical techniques. The β-glucosidase immobilized on a CS-MIL-Fe composite had an immobilization yield of 85 % and a recovered activity of 74 %. The immobilized enzyme retained 81 % of its initial activity after ten successive cycles and preserved 69 % of its original activity after 30 days of storage at 4 °C. In contrast, the free enzyme had only preserved 32 % of its original activity after 30 days. Under various temperature and pH conditions, the immobilized enzyme showed greater stability than the free enzyme, and the optimal temperature and pH were 60 °C and 6.0 for the immobilized enzyme and 50 °C and 5.0 for the free enzyme. The kinetic parameters were also determined, with the Km values of 13.4 and 6.98 mM for the immobilized and free β-glucosidase, respectively, and Vmax values of 3.96 and 1.72 U/mL, respectively. Overall, these results demonstrate that the CS-MIL-Fe@β-glucosidase is a promising matrix showing high catalytic efficiency and enhanced stability.

1. Introduction

The main principles of sustainability (green chemistry) emphasize catalyst production and the development and optimization of catalysts for sustainable production. Optimal catalysts reduce waste generation and energy consumption while increasing output and simplifying the syntheses of desired products [1,2]. Because of their distinctive qualities, such as high activities and selectivities, biocatalysts are among the most adaptable catalysts [3,4]. Enzymes have catalytic properties; but, they also have numerous drawbacks. One notable challenge is in practical utilization of free enzymes on industrial scales. They are also unstable and cannot be employed for several cycles. Immobilizing enzymes in solid materials is one of the most popular and intriguing methods for overcoming these constraints [5,6]. Immobilized enzymes offer numerous advantages, including improved stability, reusability, activity,

☆ Mustafa Zeyadi reports financial support was provided by King Abdulaziz University. Mustafa Zeyadi reports a relationship with King Abdulaziz University that includes: employment.

* Corresponding authorDepartment of Chemistry, College of Science and Arts at Khulis, University of Jeddah, Jeddah 21921, Saudi Arabia.
E-mail address: yaseralmoliki@hotmail.com (Y.Q. Almulaiky).

https://doi.org/10.1016/j.heliyon.2023.e21169
Received 10 August 2023; Received in revised form 13 October 2023; Accepted 17 October 2023
Available online 18 October 2023

and selectivity, as well as simplified product separation. Immobilization techniques prevent subunit dissociation, reduce aggregation, autolysis, or proteolysis, enhance enzyme rigidification, and create favourable microenvironments, ultimately leading to increased enzyme stability [7–9]. Various materials, such as nanocomposites, metal organic frameworks, and polymers, are commonly employed for immobilization [10–12]. However, there are certain drawbacks associated with immobilized enzymes, such as reduced enzyme loadings, diffusion limitations, potential loss of enzyme activity, and increased costs and complexity [13]. To address these limitations, recent studies have been focused on enzyme-shielding strategies. For example, researchers have successfully shielded immobilized lipase on silica nanospheres by applying a porous silica layer through silane self-assembly and polycondensation, effectively protecting the enzyme from protease degradation [14].

In this study, β-glucosidase immobilization was investigated due to its importance in various biotechnological applications. The β-glucosidase enzyme plays a crucial role in the hydrolysis of β-glycosidic bonds and catalyses the conversion of cellobiose and other β-glucosides into glucose. This enzyme is of particular interest in industries such as biofuel production, food processing, and pharmaceuticals, where efficient conversion of complex sugars is essential [15].

The choice of a solid support is the key factor in enzyme immobilization [16,17]. The support must have a large surface area, particular functional groups, be stable, inactive, suitable for enzymes, stable toward deformation, abrasion, and microbial attack, and be easily accessible and affordable [18]. Nanomaterials are among the primary materials that can open new opportunities for researchers. Nanomaterials and enzymes have been combined to form a new discipline known as nanobiocatalysis. This is because nanobased materials have remarkable properties such as high adsorption capacities, great stabilities, significant surface areas, reusability and facile modifications [19].

Metal-organic frameworks (MOFs) are some of the many resources that can be utilized as supports for immobilized enzymes. MOFs exhibit distinct advantages over conventional mesoporous materials due to their uniform permeabilities and significantly expanded exterior areas resulting from their composition with metal nodes and organic linkers. Due to their special qualities, which include structural flexibility, customizable high porosity, large surface area, and the potential for postsynthetic modification, their use as immobilization supports has been promoted. The powdery forms of MOFs present significant constraints in utilization as adsorption agents in various application domains. They have limited recycling potential, difficult fabrication methods, and provide the possibility of secondary contamination because of their crystalline forms. Immobilizing enzymes on MOFs offers advantages such as high enzyme loading capacities, improved stability and protection, enhanced selectivities and specificities, and tunable properties. However, there are also disadvantages to consider, including diffusion limitations, synthetic complexity, and the potential loss of enzyme activity [20,21]. One approach to overcoming these limitations, is to immobilize the MOFs on a solid material such as fibers, polyacrylamide, cotton, or membranes [22–25]. Polymers are commonly used as carriers to incorporate MOFs and create shaped porous materials [26]. However, creating low-cost supports for adsorbent materials remains necessary. "Bioadsorbents derived from sustainable and natural polymers have become increasingly popular in the field of adsorption, particularly due to their cost-effectiveness, environmental sustainability, and safety [27]. The incorporation of MOFs has been studied with alginate and cellulose as patterns, as reported in Ref. [28]. Chitosan, a polysaccharide composed of N-acetyl-D-glucosamine and D-glucosamine and obtained through chitin deacetylation, is among the most extensively researched natural polymers. Due to the presence of active amino and hydroxyl functional groups that could create crosslinks with enzymes, chitosan has undergone substantial study as a potential carrier for enzymes [9,29]. Combinations of MOFs and chitosan can generate mouldable adsorbents and enhanced immobilization capabilities. To generate homogenous and stable MOFs on chitosan substrates, an effective CS-MIL-Fe composite was developed in this work for immobilizing β-glucosidase. The techniques employed in the study were scanner electron microscopy (SEM) and Fourier transform infrared (FT-IR) Spectroscopy.

1.1. Materials and methods

ııTrimesic acid (95 %), Iron (III) nitrate nonahydrate ($Fe(NO_3)_3{\cdot}9H_2O$), trimethylamine (anhydrous, ≥99 %), 4-nitrophenyl-β-D-glucopyranoside (*p*-NPG), β-glucosidase from almonds, *p*-nitrophenol, 1-ethyl-3-(3-dimethylaminopropyl) carbodiimide (EDC), N- hydroxysuccinimide (NHS), and chitosan were purchased from Merck (Darmstadt, Germany). Dimethylformamide (DMF), ethanol, and sodium hydroxide were obtained from Fisher Scientific (Hampton, NH). All chemicals were used as received and without additional purification.

1.2. Fabrication of CS- MIL-Fe composites

First, a mixture of $Fe(NO_3)_3.9H_2O$ (15 mmol) and trimesic acid (15 mmol) were dissolved in 70 mL a DMF: ethanol mixed solvent (1:1). The mixture was well blended with steady magnetic stirring then 2 mL of trimethylamine was added dropwise with continuous stirring for 2 h before being relocated to a Teflon-fitted autoclave and incubated at 80 °C for 21h. Subsequently, the response vessel was removed from the oven and allowed to reach room temperature. The final product was centrifuged to separate the MIL-Fe powder and then dried at 100 °C in an oven after being washed three times with DMF: ethanol. In this experiment, 1 g of chitosan was immersed in 50 mL of 2 % acetic acid. Following this, 2 g of MIL-Fe powder was dispersed within the chitosan solution. The mixing fluid was added dropwise to a solution of NaOH (100 mL, 1 M). Following a 3 h stirring period, the resultant CS-MIL-Fe composite underwent multiple rinses with distilled water until the resulting solution reach neutral pH.

1.3. Immobilization of β-glucosidase on CS- MIL-Fe composites

Immobilization of β-glucosidase on the CS-MIL-Fe composite was performed as follows. EDC (50 mg) was added to 10 ml of saline

phosphate buffer (50 mM PBS with pH 7.4) containing 500 mg of the CS-MIL-Fe composites and incubated for 1 h at room temperature with constant stirring. Subsequently, 50 mg of N-hydroxysuccinimide (NHS) was introduced into the solution, which was subjected to continuous agitation for 1.5 h at ambient temperature. Subsequently, the solution was transferred to a Falcon tube that contained 10 mg of β-glucosidase in 10 mL of PBS. The immobilization process was carried out by end-over-end rotation for 12 h at ambient temperature. The sample was centrifuged to facilitate separation, followed by two washes with phosphate buffered saline. Utilizing bovine serum albumin for comparison, the Bradford method [30] was used to calculate the amount of protein loaded. The following formulae were applied:

Immobilization Yield (IY%) = .

$$\frac{\text{Amount of protein introduced} - \text{Protein in the supernatant}}{\text{Amount of protein introduced}} \text{ X } 100 \quad (1)$$

$$\text{Activity yield (AY\%)} = \frac{\text{Immobilized enzyme activity}}{\text{Iniatial activity}} \text{ X } 100 \quad (2)$$

1.4. β-Glucosidase activity assay

Using the substrate *p*-NPG, Narasimha's approach was used to estimate the liberation of *p*-nitrophenol and determine the activity of the β-glucosidase [31]. In summary, 0.9 mL of 5 mM *p*-NPG in 0.1 M acetate buffer (pH 6.0) was added to 0.1 mL of free β-glucosidase or 10 mg of immobilized β-glucosidase. Then, 0.5 mL of a1 M Na_2CO_3 solution was added to the reaction mixture to stop the reaction after incubation for 5 min at 37 °C. The absorbance at 405 nm was then measured. One unit of β-glucosidase activity was defined as the amount of enzyme that produced 1 μmol of *p*-nitrophenol/min."

1.5. Material characterization

The present study utilized scanning electron microscopy in conjunction with energy dispersive X-ray spectroscopy (SEM, Quanta FEG 250, FEI Co., Hillsboro, USA) to investigate the morphological structure and elemental composition of the material support. The functional groups of the CS-MIL-Fe composite were analysed with Fourier-transform infrared spectroscopy (FTIR, PerkinElmer Spectrum 100) both prior to and subsequent to immobilization of the enzymes. The zeta potentials of the samples were determined with dynamic light scattering (Entgris, Nicomp Nano Z3000, Billerica, MA, USA)."

1.6. Operational stability of biocatalyst

To determine the operational stability of the immobilized enzyme, "a known quantity of CS-MIL-Fe@β-glucosidase was introduced into a reaction tube containing the substrate solution, and the reaction was carried out under ideal circumstances. To remove the CS-MIL-Fe@β-glucosidase from the reaction mixture, the mixture was centrifuged and washed with 0.1 M acetate buffer, pH 6.0." After washing, the CS-MIL-Fe@β-glucosidase was repeatedly used by including new substrate. The relative activity was considered to be 100 % in the initial application.

1.7. Thermal and storage stability

In actuality, thermal inactivation poses a significant obstacle for industrial enzymes. The 3D structure of the enzyme is altered by exposure to high temperatures. Following preincubation for 120 min at a temperature of 50 °C, assessments were conducted to determine how stable both enzymes were. After a 30-min incubation period, samples of the enzyme were collected and the residual activity percentage was determined. The enduring stability during storage was assessed for both the free and immobilized enzymes by subjecting them to a 30-day incubation period at a temperature of 4 °C. The residual activity was measured by withdrawing specimens at various times and the initial activity was designated as 100 %.

1.8. Optimization of pH and temperature

"To investigate the impact of temperature on the enzyme activity, experiments were conducted wherein both free and immobilized β-glucosidase were incubated with substrate at varying temperatures ranging from 30 to 80 °C for a duration of 15 min. The measurements of β-glucosidase activities were carried out as described in the activity assay section. Furthermore, the effects of pH on the activities of the free and immobilized β-glucosidase were determined. This was achieved by subjecting samples to varying pHs (ranging from 4.0 to 8.5)" for 15 min, after which the β-glucosidase activities were assessed. The optimal activity achieved at the given pH and temperature was regarded as 100 %, and the enzyme activity in each test was normalized to that relative activity.

1.9. Kinetic parameters

The steady-state velocities of the enzyme reaction were measured while increasing the concentration of *p*-NPG from 3 mM to 5.5 mM in acetate buffer (pH 6, 0.1 M), and the Michelis–Menten constant (Km) and the maximum rate (Vmax) of the β-glucosidase

reaction were determined. The Lineweaver–Burk equation was used to establish double reciprocal plots for the Km and Vmax values."

1.10. Effect of organic solvent

The effect of organic solvents on the β-glucosidase activity were investigated with 20 % (v/v) methanol, ethanol, dimethyl sulfoxide (DMSO), and isopropanol. Before investigating the enzyme activity, the enzyme was incubated in the organic solvent for 30 min.

2. Results and discussion

MIL-Fe was synthesized via a solvothermal reaction. Then to improve the efficiency of the material support in enzyme immobilization, the MIL-Fe was blended with chitosan. The synthesis and structure of the CS-MIL-Fe composite is shown in Fig. 1 and S. The uniform dispersion of metal ions within the chitosan was attributed to coordination between the amino groups in chitosan and the metal ions. The SEM image (Fig. 3b) provided visual evidence for uniform dispersion of the metal ions within the chitosan. The metal oxide and chitosan composite was formed by the blending liquid droplets with an alkali solution (NaOH) owing to the insolubility of chitosan. The MIL-Fe created in the previous stage was consistently dispersed throughout the chitosan matrix. Fe $(NO_3)_3$ $9H_2O$ was chosen to create a metal ion/chitosan blending solution for manufacture of the CS-MIL-Fe composites. CS-MIL-Fe@β-glucosidase was successfully prepared through immobilization of almond β-glucosidase onto the CS-MIL-Fe composite via covalent cross-linking. The β-Glucosidase was immobilized on the CS-MIL-Fe composite with an immobilization yield of 85 % and a recovered activity of 74 %. In the literature, β-glucosidase immobilized on a modified polyester exhibited an enzyme activity of 82.3 % and an immobilization yield of 89.5 % [16]. Zheng et al. [32] showed that β-glucosidase wasimmobilized on magnetic chitosan microspheres with an immobilization efficiency of 90.2 %. The successful immobilization of the β-glucosidase may have resulted from permanent crosslinking of the enzyme and carrier by EDC/NHS, as suggested by immobilization of the enzyme via strong covalent binding to CS-MIL-Fe. The enzyme efficacy was improved as the steric barriers surrounding the enzyme active sites were reduced due to the large surface area of the carrier and dispersion of the enzyme [33,34]. The robust chemical linkages between MOFs and enzymes are thought to involve covalent bonds [35]. The stable arrangement of numerous covalent bonds between MOFs and enzymes might substantially minimize the structural flexibility and consolidate the enzymes to prevent proteins from leaking, unfolding, collapsing, or denaturing [35,36].

2.1. FTIR characterization

Fig. 2 shows the FTIR spectra of MIL-Fe, the CS-MIL-Fe composite, and CS-MIL-Fe@β-glucosidase. The presence of organic compounds and new functional groups were confirmed by the FTIR spectrum of the as-produced MIL-Fe. The strong bands at 3458 cm^{-1} and 2852 cm^{-1} arose from stretching vibrations of O–H and C–H bonds, respectively. Two significant peaks at 1653 cm^{-1} and 1378 cm^{-1} were attributed to the symmetric and asymmetric stretching modes of coordinated (COO-) groups, respectively. The uncoordinated, free carboxyls on the surface of MIL-Fe were responsible for the weak peak at 1286 cm^{-1} which was assigned to C–O stretching vibrations. The band at 661 cm^{-1} was assigned to stretching vibrations of aromatic C–H and O–H bonds. These bands shifted, and there were noticeable differences in their intensities after subsequent treatments. The characteristic peak for chitosan at 3448 cm^{-1} was

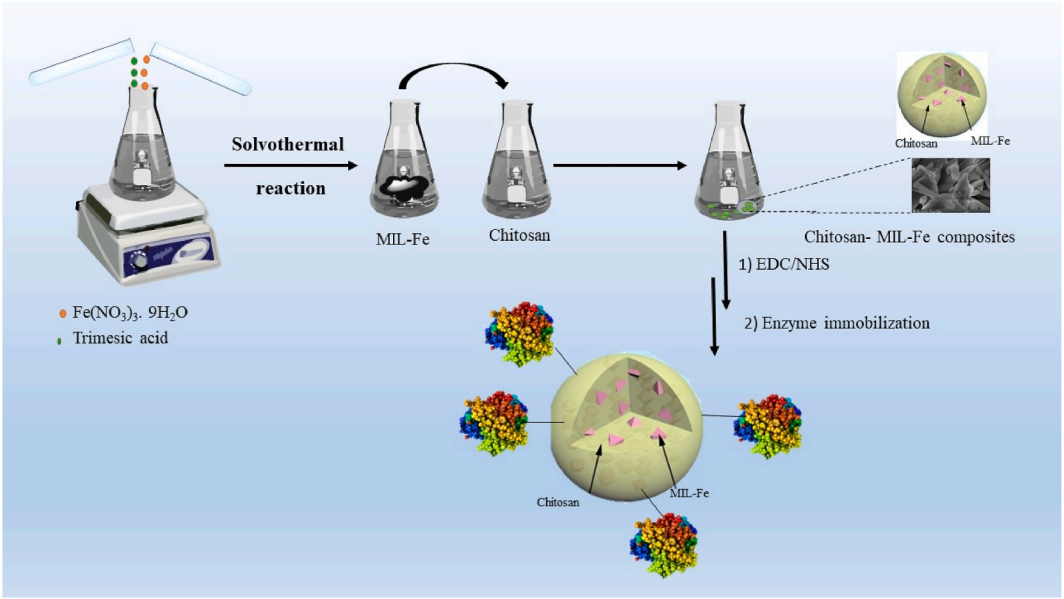

Fig. 1. The synthesis of chitosan- MIL-Fe composites and enzyme immobilization.

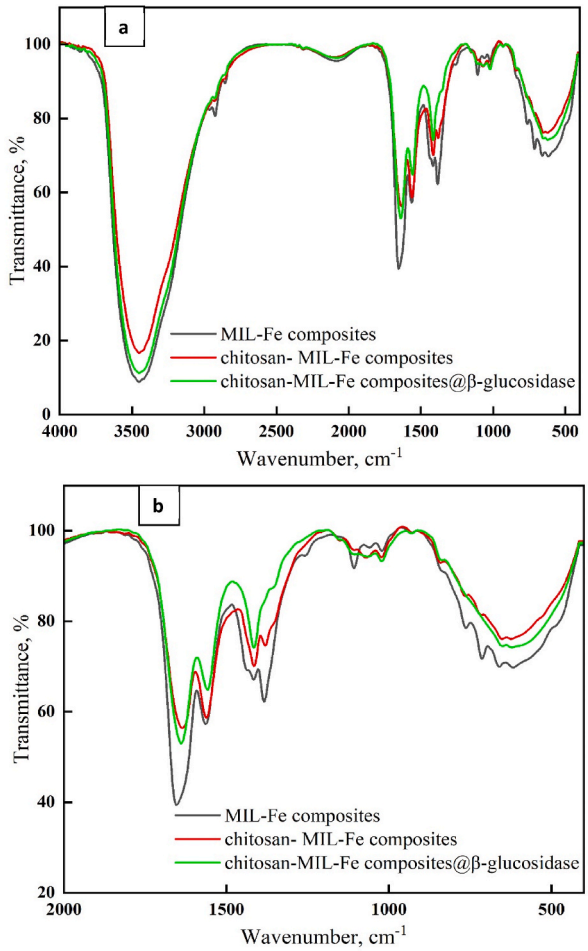

Fig. 2. ATR-FT-IR spectra of MIL-Fe, CS- MIL-Fe composites, and CS- MIL-Fe composites@ β-glucosidase (a: full scale and b: expanded scale).

attributed to overlapping peaks for O–H and NH_2 stretching vibrations. The carbonyl stretching (amide 1 band) and asymmetric N_H stretching vibration gave peaks at approximately 1639 cm^{-1} and 1553 cm^{-1}. Additionally, the presence of β-glucosidase was evidenced by changes in the substrate bands after enzyme immobilization, as well as peak at 1024 cm^{-1} for the glycosidic (C–*O*–C) linkage. The intensities of peaks changed after enzyme immobilization, confirming the successful enzyme immobilization [10,29].

2.2. Morphological characterization

The surface morphological changes to the metal organic frameworks brought on by the chemical treatments were examined with scanning electron microscopy. The morphological structures of MIL-Fe, the CS-MIL-Fe composite and the CS-MIL-Fe@β-glucosidase are shown in Fig. 3. Fig. 3a shows that the MIL-Fe particles were regularly distributed spherical agglomerates. Blending of the chitosan and MIL-Fe resulted in a rod-like morphology for the CS-MIL-Fe composite (Fig. 3b). After enzyme immobilization, the surface exhibited wavy clumps without pores as shown in Fig. 3c. The incorporation of CS modified the crystal growth process and influenced the overall morphology of the material. Additionally, the interaction between CS and MIL-Fe may have caused structural rearrangements and changes in the particle sizes or shapes. Furthermore, enzyme immobilization often involves surface interactions that can affect the distribution and arrangement of particles in the composite.

The EDX technique used to determine the chemical compositions of bulk materials by generating X-rays that penetrate the surface to a depth of approximately 2 μm [37]. Fig. 4 and the accompanying data reveal that CS-MIL-Fe@β-glucosidase contained 56.55 % and 2.35 % carbon and iron by weight, respectively.

2.3. Zeta potential and intensity-weighted mean hydrodynamic size

In addition to the chemical properties of the enzyme and carrier, the effectiveness of enzyme immobilization was determined from the surface potential of the carrier. The zeta potential is assumed to indicate the efficacy of enzyme binding since it indicates

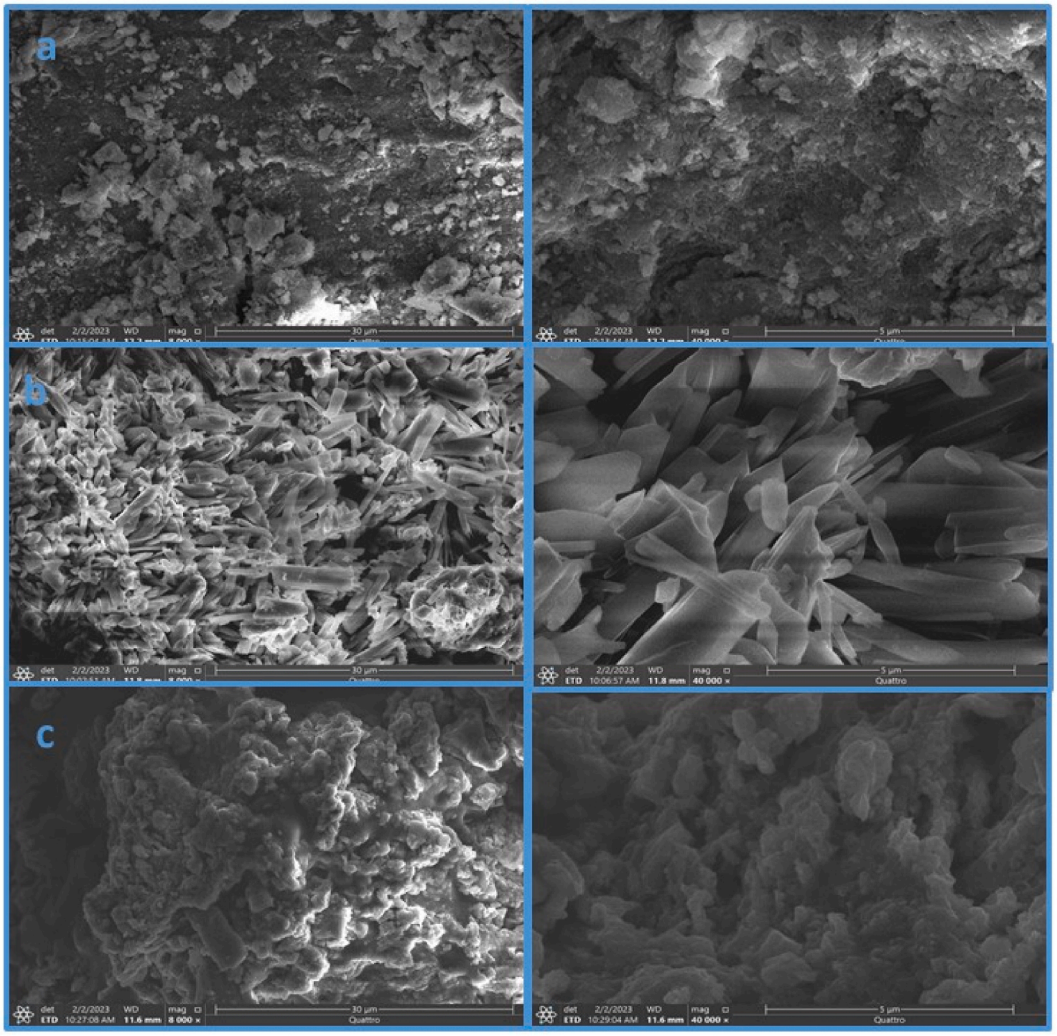

Fig. 3. FESEM images of MIL-Fe (a), CS- MIL-Fe composites (b), and CS- MIL-Fe@ β-glucosidase (c).

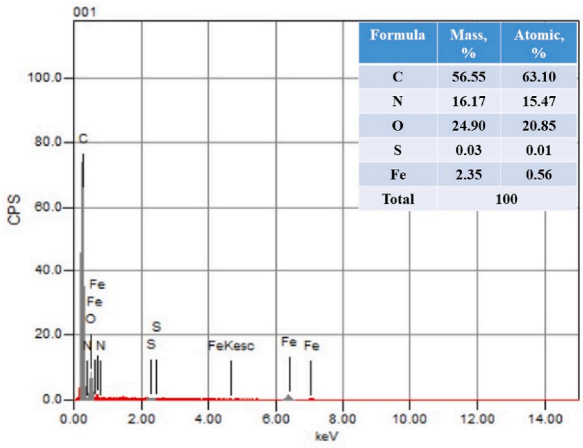

Formula	Mass, %	Atomic, %
C	56.55	63.10
N	16.17	15.47
O	24.90	20.85
S	0.03	0.01
Fe	2.35	0.56
Total	100	

Fig. 4. The SEM–energy-dispersive X-ray (EDX) spectra of CS-MIL-Fe composites@β-glucosidase

electrostatic interactions between the support and the enzyme [11,38]. The zeta potentials of the materials under study are shown in Table 1, the zeta potential of MIL-Fe was −29.1 mV," but, after blending with chitosan, it increased to −6.65 mV. This could be because chitosan contains amino groups. The zeta potential plummeted to −15.5 mV after the enzyme was immobilized, which may have been caused by electrostatic interactions between the support and the ionizable groups of the enzyme. Immobilization reduced of the general surface charge, contingent upon the enzyme charge. The changes in the functional groups and surface features impacted the zeta potentials. The outcomes described above indicated that the surface modifications and immobilization of β-glucosidase were effectively executed. Furthermore, as indicated in Table 1, the intensity-weighted mean hydrodynamic size (Z-Average) of the sample under study was analysed. The Z-average for MIL-Fe was 80 d nm. After blending with chitosan, the Z-average was increased to 1958 d nm. It is possible that chitosan, which has NH_2 groups to interact with water molecules, was responsible for the increase in Z-average. β-Glucosidase immobilization increased the Z-average to 2339 d nm. The inclusion of chitosan and β-glucosidase, which have hydrophilic groups that interact with water probably led to these variations in the average hydrodynamic diameters. These results were consistent with other results [39,40].

2.4. Operational stability of the immobilized enzyme

The potential for reuse important in both commercial and industrial contexts. Immobilization has the potential to reduce the overall cost of the enzyme, as it facilitates repeated utilization in batch-specific activities. After recycling for five cycles, as shown in Fig. 5, 93 % of the original activity was maintained. After ten cycles, 81 % of the original activity was determined. Enzyme structural alterations or adsorption of the substrates and products, which affect the reaction sites, may have decreased the activity during repeated cycling [41,42]. This is consistent with previous studies showing that sodium alginate-coated magnetic nanoparticles [43] and modified polyester [16] used as β-glucosidase carrier supports maintained 39.5 % and 82 % of the original activities after 10 and 6 cycles, respectievly.

2.4.1. Thermal and storage stability

Thermal stability is an important parameter affecting the use of an immobilized enzyme. Fig. 6a shows the fluctuating activity levels remaining after incubation for 120 min at 50 °C and 60 °C. Both the free and immobilized forms of β-glucosidase showed activity declines, and the free form experienced a greater decline than the immobilized form. The immobilized β-glucosidase retained 48 % of its initial activity after 120 min of incubation, while free β-glucosidase only retained 21 % of its initial activity at 50 °C. At 60 °C, the immobilized and free enzyme showed 81 and 54 % of their initial activities, respectively, after 120 min. The rigidity of the β-glucosidase tertiary structure arising from multiple interactions with the support may have affected the stability of the immobilized β-glucosidase during incubation at high temperatures [44]. All of the β-glucosidase samples were maintained at 4 °C for 30 days, and the activities were evaluated every 5 days (Fig. 6b). The immobilized β-glucosidase preserved 69 % of its original activity, whereas free β-glucosidase retained 32 % of its original activity. In a previous study by Sanchez-Ramirez et al. [45], it was shown that cellulase immobilized on chitosan-magnetic nanoparticles retained 50 % of its activity after 4 h at temperatures of 60 °C and 70 °C. Similarly, Pota et al. [46] demonstrated that β-glucosidase immobilized on wrinkled SiO_2 nanoparticles exhibited slightly enhanced stability when incubated at 70 °C. Furthermore, Wan et al. [47] showed that β-glucosidase immobilized on a Fe_3O_4@POP composite displayed improved thermal stability at 70 °C. These results indicated that the immobilized β-glucosidase had substantially greater storage stability than the free form. The enhanced stability of the immobilized enzyme was due to covalent binding with the chitosan-MIL-Fe composite via crosslinking with EDC/NHS, resulting in a more stable enzyme configuration. Furthermore, the pore structure and microenvironment of the chitosan-MIL-Fe composite inhibited enzyme aggregation, promoted enzyme stability, and sustained enzyme activity.

2.5. Effects of pH and temperature

The structural configurations of enzymes are impacted by pH variations. The enzyme can become inactive due to irreversible structural deformations caused by extreme pHs. Furthermore, this could ionize the enzyme's active centres in solution, thereby influencing the catalytic efficiency of the enzyme. The impacts of pH on the free and immobilized β-glucosidase were determined, as depicted in Fig. 7a. The immobilized enzyme exhibited its highest level of activity at a pH of 6.0, whereas the unbound enzyme demonstrated its peak activity at a pH of 5.5. The observed difference may have arisen from ion exchange between the medium and the enzyme. The optimal pH of the enzyme was shifted to a higher pH by charged carriers when the concentration of cations in the vicinity of the carrier surface surpassed that of the solution. Furthermore, under alkaline conditions, the immobilized enzyme exhibited a considerably greater degree of pH stability than the soluble counterpart. The pH activity profile is often affected by unequal

Table 1
Zeta potentials and intensity weighted mean hydrodynamic size of MIL-Fe, CS-MIL-Fe composites and CS-MIL-Fe@β-glucosidase.

Sample	Zeta potential (mV)	Z-Average (d.nm)
MIL-Fe	−29.1	503.6
CS-MIL-Fe composites	−6.65	1958
CS-MIL-Fe@β-glucosidase	−15.5	2339

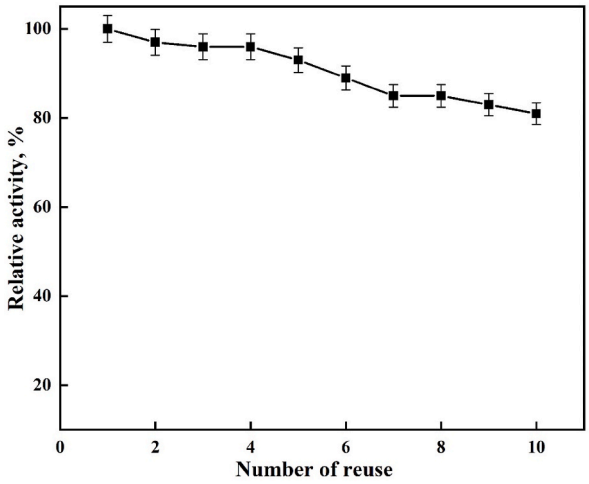

Fig. 5. Reusability of immobilized enzyme.

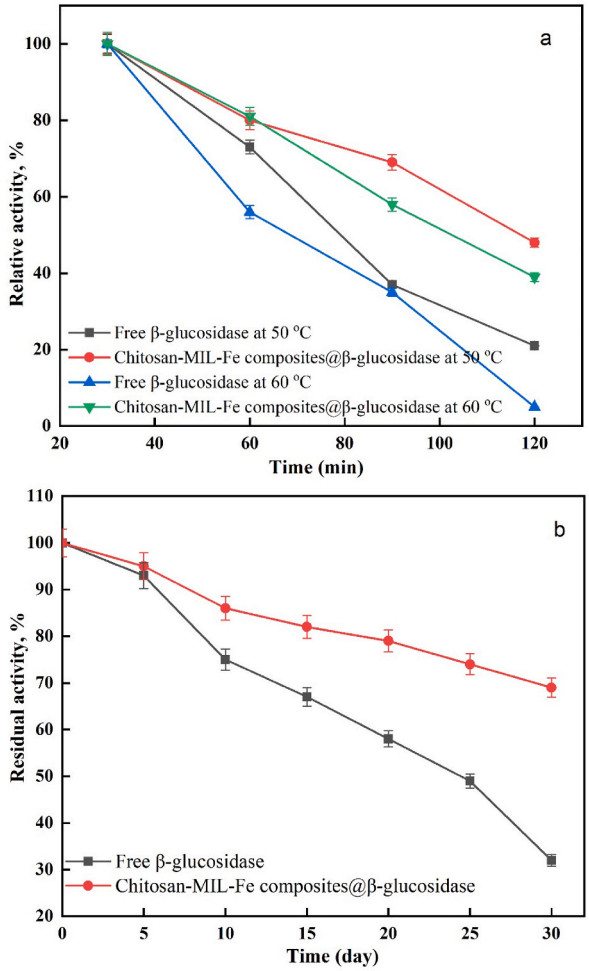

Fig. 6. Thermal stability (a) and storage stability (b) of free and immobilized enzymes.

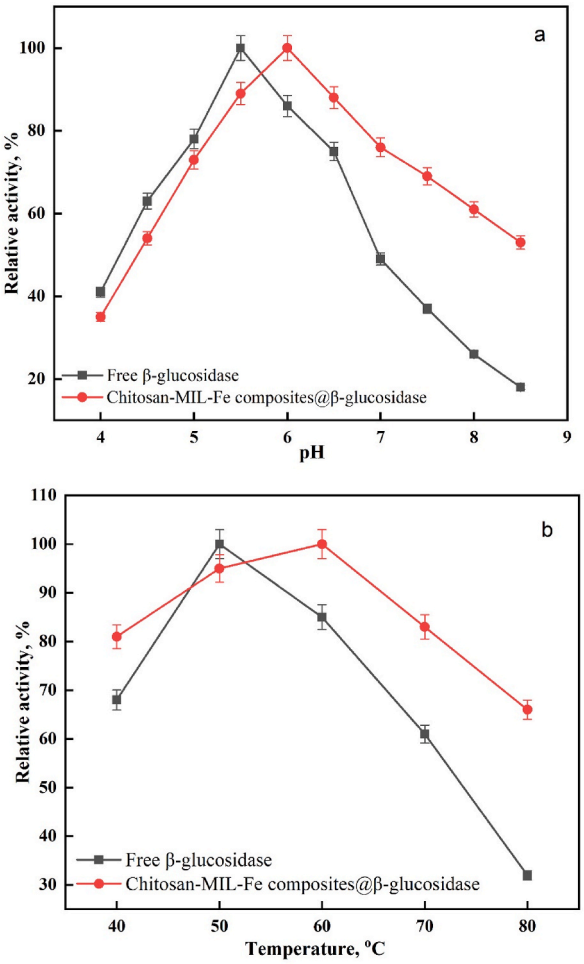

Fig. 7. Effect of pH (a) and temperature (b) on the activity of free and immobilized enzymes.

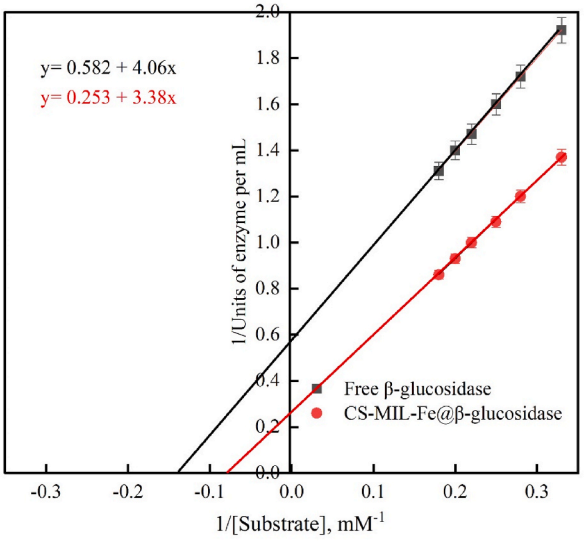

Fig. 8. Kinetic parameters of free and immobilized enzymes.

partitioning of H^+ and OH^- concentrations between the microenvironment surrounding the immobilized enzyme and the bulk solution. This discrepancy arises from electrostatic interactions with the matrix and can result in displacements [48].

The observed increase in the optimal pH for the immobilized β-glucosidase to higher pH corroborated the results of Naseer et al. [49]. Specifically, their study demonstrated that the optimal pHs for free β-glucosidase and β-glucosidase immobilized on nano-SiO_2 were 6.0 and 7.5, respectively. Gupta et al. [50] and Çelik et al. [51] determined a change in the optimal pH from 5.0 to 6.0 after β-glucosidase immobilization. The performance of both the free and immobilized β-glucosidase was evaluated with a series of working solutions that were subjected to varying temperatures ranging from 40 to 80 °C. The activity profiles of the free and immobilized β-glucosidase are presented in Fig. 7b. The optimal activities for the free and immobilized β-glucosidase was observed at 50 °C and 60 °C. The thermal stability of the β-glucosidase enzyme was enhanced through covalent immobilization on the CS-MIL-Fe composite. The immobilized β-glucosidase exhibited a higher residual activity at temperatures exceeding 60 °C than the free β-glucosidase, indicating its superior thermal stability. The robust interplay between β-glucosidase and the CS-MIL-Fe composite prevented denaturation of the active catalyst. This was achieved by restricting the conformational changes that may have occurred within the β-glucosidase subjected to elevated temperatures [16]. Various researchers have shown that the optimal temperature shifted after immobilized β-glucosidase. One such study conducted by Naseer et al. [49] showed a temperature change from 50 to 70 °C for β-glucosidase immobilized on nano-SiO_2. According to Patel et al. [52], the optimal temperature for both soluble and immobilized β-glucosidase was 60 °C.

2.6. Kinetic behaviour

The present study investigated the effects of substrate concentrations on the catalytic activities of free and immobilized β-glucosidase by utilizing varying amounts of pNPG as the substrate (as depicted in Fig. 8). A Lineweaver−Burk plot was prepared to determine the constant kinetic (km) and maximum reaction velocity (Vmax) for both the free and immobilized enzymes. The immobilized enzyme exhibited a km value of 13.4 mM, which was higher than that of the free β-glucosidase (km = 6.98 mM). In general, immobilization may increase enzyme resistance to the substrate and, as a result, raise the km value because immobilization restricted access to the enzyme active site [46]. Califano et al. [53] and Verma et al. [54] highlighted the potential influence of diffusion limitations on the km observed for the immobilized enzyme. On the other hand, the morphology of the host material (CS-MIL-Fe) could contribute diffusion constraints and affect the enzyme-substrate interactions.

In addition, the immobilized β-glucosidase (Vmax = 3.96 U/mL) showed a higher Vmax than the free form (Vmax = 1.72 U/mL). This could be attributed to a rise in the substrate concentration within the bulk solution, leading to acceleration of substrate diffusion towards the enzyme, which may eventually reach a threshold level. If an immobilized enzyme attains the maximum velocity (Vmax) only after achieving complete substrate saturation, then the Vmax value will be higher than that of the enzyme in free solution [46]. Supporting materials offer solvent resistance and stability for enzymes. After incubation, free β-glucosidase exhibited a substantial decline in relative activity, which decreased from 69 % to 12 % in the order isopropanol > ethanol > methanol > DMSO, (Table 2). In comparison with the free enzyme, CS-MIL-Fe@β-glucosidase maintained higher relative activities in the presence of solvents and demonstrated higher solvent tolerance with ranges of 87–61 %. These findings indicated that CS-MIL-Fe@β-glucosidase could be suitable for large-scale application.

3. Conclusion

In this study, β-glucosidase from almonds was immobilized on a CS-MIL-Fe composite. FTIR, SEM, EDX, and zeta potential measurements confirmed covalent immobilization of the enzyme on the CS-MIL-Fe composite. The β-Glucosidase immobilized on the CS-MIL-Fe composite exhibited a recovered activity of 74 % with an immobilization yield of 85 %. The immobilized β-glucosidase preserved 81 % of its original activity after being reused ten times. The immobilized β-glucosidase tolerated broader pH and temperature ranges and showed improved thermal and storage stability. These results suggest that the CS-MIL-Fe composite could be a viable alternative for loading of various enzymes and widespread application. The potential for commercial use of enzymes will expand with the use of responsive architectures, which will provide significant enhancement in enzymatic stability. The outcomes from this study will guide future designs of more sophisticated transport and delivery systems for use with drug/enzyme-loaded responsive polymeric systems.

Funding

This research work was funded by Institutional Fund Projects under no. (IFPIP: 485-130-1443). The author gratefully acknowledge technical and financial support provided by the Ministry of Education and King Abdulaziz University DSR, Jeddah, Saudi Arabia.

Ethics

Not applicable.

Availability of data

Data generated and utilized for analyses of results presented in this manuscript are available from the corresponding author on

Table 2
Effect of organic solvents on the activity of free β-glucosidase and CS-MIL-Fe@β-glucosidase.

Solvents 20 % (v/v)	Relative activity (%)	
	Free β-glucosidase	CS-MIL-Fe@β-glucosidase
Isopropanol	69 ± 1.02	87 ± 1.53
Ethanol	34 ± 0.87	62 ± 0.85
Methanol	18 ± 0.02	65 ± 0.88
DMSO	12 ± 0.59	61 ± 0.37

reasonable requests.

Data availability statement

Data will be made available on request.
No additional information is available for this paper.

CRediT authorship contribution statement

Mustafa Zeyadi: Formal analysis, Data curation, Conceptualization. **Yaaser Q. Almulaiky:** Writing – review & editing, Writing – original draft, Visualization, Validation, Resources, Project administration, Methodology, Investigation.

Declaration of competing interest

The authors declare the following financial interests/personal relationships which may be considered as potential competing interests.

References

[1] H.C. Erythropel, J.B. Zimmerman, T.M. deWinter, L. Petitjean, F. Melnikov, C.H. Lam, A.W. Lounsbury, K.E. Mellor, N.Z. Janković, Q. Tu, L.N. Pincus, M. M. Falinski, W. Shi, P. Coish, D.L. Plata, P.T. Anastas, The Green ChemisTREE: 20 years after taking root with the 12 principles, Green Chem. 20 (2018) 1929–1961.
[2] F. Amin, A. Mohsin, H.N. Bhatti, M. Bilal, Production, thermodynamic characterization, and fruit juice quality improvement characteristics of an exopolygalacturonase from Penicillium janczewskii, Biochim. Biophys. Acta Protein Proteonomics 1868 (2020), 140379.
[3] E.M.M. Abdelraheem, H. Busch, U. Hanefeld, F. Tonin, Biocatalysis explained: from pharmaceutical to bulk chemical production, React. Chem. Eng. 4 (2019) 1878–1894.
[4] M. Bilal, N. Hussain, J.H.P. Américo-Pinheiro, Y.Q. Almulaiky, H.M. Iqbal, Multi-enzyme co-immobilized nano-asse mblies: bringing enzymes together for expanding bio-catalysis scope to meet biotechnological challenges, Int. J. Biol. Macromol. 186 (2021) 735–749. .
[5] A.R. Silva, J.Y. Alexandre, J.E. Souza, J.G.L. Neto, P.G. de Sousa Júnior, M.V. Rocha, J.C. Dos Santos, The chemistry and applications of metal–organic frameworks (MOFs) as industrial enzyme immobilization systems, Molecules 27 (14) (2022) 4529.
[6] J. Gan, A.R. Bagheri, N. Aramesh, I. Gul, M. Franco, Y.Q. Almulaiky, M. Bilal, Covalent organic frameworks as emerging host platforms for enzyme immobilization and robust biocatalysis–A review, Int. J. Biol. Macromol. 167 (2021) 502–515. .
[7] Z. Wang, R. Wang, Z. Geng, X. Luo, J. Jia, S. Pang, J. Cui, Enzyme hybrid nanoflowers and enzyme@ metal–organic frameworks composites: fascinating hybrid nanobiocatalysts, Crit. Rev. Biotechnol. (2023) 1–24. .
[8] G. Kuang, Z. Wang, X. Luo, Z. Geng, J. Cui, M. Bilal, S. Jia, Immobilization of lipase on hydrophobic MOF synthesized simultaneously with oleic acid and application in hydrolysis of natural oils for improving unsaturated fatty acid production, Int. J. Biol. Macromol. 242 (2023).
[9] Y.Q. Almulaiky, N.M. Khalil, Y. Algamal, A. Al-Gheethi, A. Aissa, S.M. Al-Maaqar, R.M. El-Shishtawy, Optimization of biocatalytic steps via response surface methodology to produce immobilized peroxidase on chitosan-decorated AZT composites for enhanced reusability and storage stability, Catal. Lett. (2022) 1–15. .
[10] Y.Q. Almulaiky, N.M. Khalil, Y. Algamal, A. Al-Gheethi, A. Aissa, S.M. Al-Maaqar, R.M. El-Shishtawy, Optimization of biocatalytic steps via response surface methodology to produce immobilized peroxidase on chitosan-decorated AZT composites for enhanced reusability and storage stability, Catal. Lett. (2022) 1–15. .
[11] R.M. El-Shishtawy, Y.M. Al Angari, M.M. Alotaibi, Y.Q. Almulaiky, Acrylic fabric and nanomaterials to enhance α-amylase-based biocatalytic immobilized systems for industrial food applications, Int. J. Biol. Macromol. 233 (2023).
[12] J. Cui, S. Ren, T. Lin, Y. Feng, S. Jia, Shielding effects of Fe3+-tannic acid nanocoatings for immobilized enzyme on magnetic Fe3O4@ silica core shell nanosphere, Chem. Eng. J. 343 (2018) 629–637. .
[13] Z.Y. Zhao, J. Liu, M. Hahn, S. Qiao, A.P. Middelberg, L. He, Encapsulation of lipase in mesoporous silica yolk–shell spheres with enhanced enzyme stability, RSC Adv. 3 (44) (2013) 22008–22013. .
[14] Z. Zhang, Y. Du, G. Kuang, X. Shen, X. Jia, Z. Wang, J. Cui, Lipase-Ca2+ hybrid nanobiocatalysts through interfacial protein-inorganic self-assembly in deep-eutectic solvents (DES)/water two-phase system for biodiesel production, Renew. Energy 197 (2022) 110–124. .
[15] A. Ahmed, K. Batool, A. Bibi, Microbial β-glucosidase: sources, production and applications, Journal of Applied & Environmental Microbiology 5 (1) (2017) 31–46.
[16] Y.Q. Almulaiky, Polyester Fabric Modification by Chemical Treatment to Enhancing the β-glucosidase Immobilization, Heliyon, 2022.
[17] M. Bilal, H.M. Iqbal, Chemical, physical, and biological coordination: an interplay between materials and enzymes as potential platforms for immobilization, Coord. Chem. Rev. 388 (2019) 1–23.
[18] R.C. Rodrigues, J.J. Virgen-Ortíz, J.C.S. dos Santos, Á. Berenguer-Murcia, A.R. Alcantara, O. Barbosa, C. Ortiz, R. Fernandez-Lafuente, Immobilization of lipases on hydrophobic supports: immobilization mechanism, advantages, problems, and solutions, Biotechnol. Adv. 37 (2019) 746–770.
[19] D. Sheng, X. Ying, R. Li, S. Cheng, C. Zhang, W. Dong, X. Pan, Polydopamine-mediated modification of ZIF-8 onto magnetic nanoparticles for enhanced tetracycline adsorption from wastewater, Chemosphere 308 (2022).
[20] Z. Wang, Y. Liu, J. Li, G. Meng, D. Zhu, J. Cui, S. Jia, Efficient immobilization of enzymes on amino functionalized MIL-125-NH2 metal organic framework, Biotechnol. Bioproc. Eng. 27 (1) (2022) 135–144. .

[21] L. Zhong, Y. Feng, H. Hu, J. Xu, Z. Wang, Y. Du, S. Jia, Enhanced enzymatic performance of immobilized lipase on metal organic frameworks with superhydrophobic coating for biodiesel production, J. Colloid Interface Sci. 602 (2021) 426–436. .
[22] X. Ma, Y. Chai, P. Li, B. Wang, Metal−organic framework films and their potential applications in environmental pollution control, Acc. Chem. Res. 52 (2019) 1461–1470.
[23] Q. Liu, K. Xu, G. Hu, F. Zeng, X. Li, C. Li, Y. Zhang, Underwater superelastic MOF/polyacrylamide/chitosan composite aerogel for efficient 2, 4-dichlorophenoxyacetic acid adsorption, Colloids Surf. A Physicochem. Eng. Asp. 635 (2022), 127970. .
[24] J. Li, Z. Yang, G. Hu, J. Zhao, Heteropolyacid supported MOF fibers for oxidative desulfurization of fuel, Chem. Eng. J. 388 (2020), 124325. .
[25] A. Yang, Z. Wang, Y. Zhu, Facile preparation and adsorption performance of low-cost MOF@ cotton fibre composite for uranium removal, Sci. Rep. 10 (1) (2020) 1–10. .
[26] K. Dong, Z. Wang, Y. Zhang, J. Ren, X. Qu, Metal–organic framework-based nanoplatform for intracellular environment-responsive endo/lysosomal escape and enhanced cancer therapy, ACS Appl. Mater. Interfaces 10 (38) (2018) 31998–32005. .
[27] M. da Silva Pinto, C.A. Sierra-Avila, J.P. Hinestroza, In situ synthesis of a Cu-BTC metal–organic framework (MOF 199) onto cellulosic fibrous substrates: cotton, Cellulose 19 (5) (2012) 1771–1779. .
[28] Y. Wang, H. Shaghaleh, Y.A. Hamoud, S. Zhang, P. Li, X. Xu, H. Liu, Synthesis of a pH-responsive nano-cellulose/sodium alginate/MOFs hydrogel and its application in the regulation of water and N-fertilizer, Int. J. Biol. Macromol. 187 (2021) 262–271. .
[29] R.M. El-Shishtawy, N.S. Ahmed, Y.Q. Almulaiky, Immobilization of catalase on chitosan/zno and chitosan/ZnO/Fe_2O_3 nanocomposites: a comparative study, Catalysts 11 (7) (2021) 820.
[30] M.M. Bradford, A rapid and sensitive method for the quantitation of microgram quantities of protein utilizing the principle of protein-dye binding, Anal. Biochem. 72 (1976) 248–254.
[31] G. Narasimha, A. Sridevi, G. Ramanjaneyulu, B. Rajasekhar Reddy, Purification and characterization of β-glucosidase from Aspergillus Niger, Int. J. Food Prop. 19 (2016) 652–661.
[32] P. Zheng, J. Wang, C. Lu, Y. Xu, Z. Sun, Immobilized β-glucosidase on magnetic chitosan microspheres for hydrolysis of straw cellulose, Process Biochemistry 48 (4) (2013) 683–687. .
[33] E.A. Barraza-González, R. Fernández-Lafuente, D.E. Zazueta-Alvarez, J.A. Rojas-Contreras, J.L. Miranda, N.S. Cruz, P.G. Vázquez-Ortega, Immobilization of β-glucosidase from Almonds on MANAE-Agarose Supports by Using the Chemistry of Glutaraldehyde, 21(1), Revista Mexicana de Ingeniería Química, 2022 ,, p. Bio2621. Bio2621.
[34] O. Almaghrabi, Y.Q. Almulaiky, A biocatalytic system obtained via immobilization of urease onto magnetic metal/alginate nanocomposite: improving reusability and enhancing stability, Biocatal. Biotransform. (2022) 1–10. .
[35] J. Gan, A.R. Bagheri, N. Aramesh, I. Gul, M. Franco, Y.Q. Almulaiky, M. Bilal, Covalent organic frameworks as emerging host platforms for enzyme immobilization and robust biocatalysis–A review, Int. J. Biol. Macromol. 167 (2021) 502–515. .
[36] J. Cui, S. Ren, B. Sun, S. Jia, Optimization protocols and improved strategies for metal-organic frameworks for immobilizing enzymes: current development and future challenges, Coord. Chem. Rev. 370 (2018) 22–41. .
[37] A.B. Stefaniak, M.G. Duling, R.B. Lawrence, T.A. Thomas, R.F. LeBouf, E.E. Wade, M.A. Virji, Dermal exposure potential from textiles that contain silver nanoparticles, Int. J. Occup. Environ. Health 20 (2014) 220–234.
[38] S.B. Sigurdardóttir, J. Lehmann, J.C. Grivel, W. Zhang, A. Kaiser, M. Pinelo, Alcohol dehydrogenase on inorganic powders: zeta potential and particle agglomeration as main factors determining activity during immobilization, Colloids Surf. B Biointerfaces 175 (2019) 136–142. .
[39] B. Ates, A. Ulu, S. Köytepe, S.A.A. Noma, V.S. Kolat, T. Izgi, Magnetic-propelled Fe 3 O 4–chitosan carriers enhance L-asparaginase catalytic activity: a promising strategy for enzyme immobilization, RSC Adv. 8 (63) (2018) 36063–36075. .
[40] G. Dik, A. Ulu, O.O. Inan, S. Atalay, B. Ateş, A positive effect of magnetic field on the catalytic activity of immobilized L-asparaginase: evaluation of its feasibility, Catal. Lett. (2022) 1–15. .
[41] Y.M. Al Angari, Y.Q. Almulaiky, M.M. Alotaibi, M.A. Hussein, R.M. El-Shishtawy, Synthesis and characterization of aminoamidine-based polyacrylonitrile fibers for lipase immobilization with effective reusability and storage stability, Int. J. Mol. Sci. 24 (3) (2023) 1970. .
[42] W.M. Alshawafi, M. Aldhahri, Y.Q. Almulaiky, N. Salah, S.S. Moselhy, I.H. Ibrahim, S.A. Mohamed, Immobilization of horseradish peroxidase on PMMA nanofibers incorporated with nanodiamond, Artif. Cell Nanomed. Biotechnol. 46 (sup3) (2018) 973–981. .
[43] F. Alnadari, Y. Xue, N.H. Alsubhi, S.A. Alamoudi, A.S. Alwabli, D.A. Al-Quwaie, F. Pan, Reusability of immobilized β-glucosidase on sodium alginate-coated magnetic nanoparticles and high productivity applications, J. Saudi Chem. Soc. 26 (5) (2022), 101517.
[44] M.F. Asar, N. Ahmad, Q. Husain, Chitosan modified Fe3O4/graphene oxide nanocomposite as a support for high yield and stable immobilization of cellulase: its application in the saccharification of microcrystalline cellulose, Prep. Biochem. Biotechnol. 50 (5) (2020) 460–467. .
[45] J. Sanchez-Ramirez, J.L. Martinez-Hernandez, P. Segura-Ceniceros, G. Lopez, H. Saade, M.A. Medina-Morales, A. Ilyina, Cellulases immobilization on chitosan-coated magnetic nanoparticles: application for Agave Atrovirens lignocellulosic biomass hydrolysis, Bioproc. Biosyst. Eng. 40 (2017) 9–22. .
[46] G. Pota, N. Gallucci, D. Cavasso, I.R. Krauss, G. Vitiello, F. López-Gallego, V. Califano, Controlling the adsorption of β-glucosidase onto wrinkled SiO_2 nanoparticles to boost the yield of immobilization of an efficient biocatalyst, Langmuir 39 (4) (2023) 1482–1494.
[47] G.Z. Wan, X.H. Ma, L. Jin, J. Chen, Fabrication of a magnetic porous organic polymer for α-glucosidase immobilization and its application in inhibitor screening, Langmuir 2023)).
[48] S.Z. Mazlan, S.A. Hanifah, Effects of temperature and pH on immobilized laccase activity in conjugated methacrylate-acrylate microspheres, International Journal of Polymer Science (2017) 2017. .
[49] S. Naseer, J. Ouyang, X. Chen, S. Pu, Y. Guo, X. Zhang, C. Yang, Immobilization of β-glucosidase by self-catalysis and compared to crosslinking with glutaraldehyde, Int. J. Biol. Macromol. 154 (2020) 1490–1495.
[50] A. Gupta, V. Kumar, A. Dubey, A.K. Verma, Kinetic characterization and effect of immobilized thermostable β-glucosidase in alginate gel beads on sugarcane juice, Int. Sch. Res. Notices 2014 (2014).
[51] A. Çelik, A. Dinçer, T. Aydemir, Characterization of β-glucosidase immobilized on chitosan-multiwalled carbon nanotubes (MWCNTS) and their application on tea extracts for aroma enhancement, Int. J. Biol. Macromol. 89 (2016) 406–414.
[52] S.K. Patel, R.K. Gupta, V. Kumar, P. Mardina, R. Lestari, V.C. Kalia, J.K. Lee, Influence of metal ions on the immobilization of β-glucosidase through protein-inorganic hybrids, Indian J. Microbiol. 59 (2019) 370–374. .
[53] V. Califano, A. Costantini, B. Silvestri, V. Venezia, S. Cimino, F. Sannino, The effect of pore morphology on the catalytic performance of β-glucosidase immobilized into mesoporous silica, Pure Appl. Chem. 91 (10) (2019) 1583–1592. .
[54] M.L. Verma, R. Rajkhowa, X. Wang, C.J. Barrow, M. Puri, Exploring novel ultrafine Eri silk bioscaffold for enzyme stabilisation in cellobiose hydrolysis, Bioresour. Technol. 145 (2013) 302–306. .